applied sciences

MDPI

Article

Nonlinear Optimal Position Control with Observer for Position Tracking of Surfaced Mounded Permanent Magnet Synchronous Motors

Dong Hyun Ha [1,2] and Raeyoung Kim [3,*]

[1] Department of Electrical Engineering, Hanyang University, Seoul 04763, Korea; dhha@sungho.co
[2] R&D Center, Sungho Electronics Co., Ltd., Anyang-si 14059, Gyeonggi-do, Korea
[3] Division of Electrical and Biomedical Engineering, Hanyang University, Seoul 04763, Korea
* Correspondence: rykim@hanyang.ac.kr; Tel.: +82-02-2220-2897

Abstract: Previous control methods were designed based on cascade structure and consist of position and current controllers for permanent magnet-synchronous motors (PMSMs). Thus, the structures of the previous methods are necessarily complex although the stability is guaranteed. Thus, the gain tuning is difficult to obtain for the desired control performance for the PMSMs. To overcome this problem, this paper proposes a nonlinear optimal position control method with an observer to improve the position tracking performance of PMSMs. The proposed method consists of a desired state generator, controller, and nonlinear observer. The desired states and inputs are derived using the PMSM model. Then, the state feedback controller is designed based on the whole tracking error dynamics including both mechanical and electrical dynamics. The nonlinear observer is designed to estimate the velocity and load torque. The closed-loop stability is proven using the input-to-state stability. The proposed method is not designed based on the cascade structure. Furthermore, the control and observer gains are chosen using an optimal control method to obtain the desired performance for the PMSMs. This approach simplifies the design process such that the control algorithm is suitable for real-time control. The performance of the proposed method is validated via simulations and experiments.

Keywords: surface mounded permanent magnet synchronous motor; nonlinear position control; nonlinear observer; LQ method

Citation: Ha, D.H.; Kim, R. Nonlinear Optimal Position Control with Observer for Position Tracking of Surfaced Mounded Permanent Magnet Synchronous Motors. *Appl. Sci.* **2021**, *11*, 10992. https://doi.org/10.3390/app112210992

Academic Editor: Adel Razek

Received: 10 October 2021
Accepted: 15 November 2021
Published: 19 November 2021

1. Introduction

Permanent magnet-synchronous motors (PMSMs) have been widely used in variable servo system applications because of several advantages, such as the absence of external rotor excitation, high power density, and a rapid dynamic response owing to their high torque-to-inertia ratio [1–3]. Generally, a proportional-integral (PI) control method has been applied to PMSMs [4]. To improve the control performance of a PMSM, various advanced methods have been proposed. An input–output linearization-based controller was designed for PMSMs in [5]. In [6], a robust nonlinear speed control was developed based on input–output linearization. A design optimization control method was proposed for the minimization of force ripple and maximization of thrust force in a brushless permanent magnet motor in [7]. Current control loop controllers were implemented using a PI current controller as a solution for velocity control in PMSMs in [8]. A nonlinear speed-regulation controller was studied for a PMSM servo system in [9]. A model predictive current control for PMSMs was proposed for improving parameter robustness in [10]. A disturbance observer-based control method was developed for the PMSMs [11]. An effective closed-loop control that consists of motor parameter identification, current control, position control, and damping control was proposed in [12]. A model predictive controller was developed for external periodic disturbances attenuation in the PMSM [13]. An output

regulator based controller was proposed to reduce sideband harmonics for the PMSM [14]. A nonlinear control method using neural network and terminal sliding mode control was proposed for the PMSM [15]. Control methods using the combination of linear quadratic regulator (LQR) method and observer were developed [16,17].

Although these methods improve the control performance of a PMSM, they require velocity and load torque measurements. Actually, it is difficult to measure both velocity and load torque because of space and/or cost limitations. Thus, several observers were proposed to estimate the state variables for the PMSM [18–21]. However, these methods did not consider the load torque or were complex for the implementation for the PMSM. Furthermore, these methods are based on a cascade structure that consists of a mechanical dynamics controller and an electrical dynamics controller. Thus, it is difficult to choose the control gains for the mechanical and electrical dynamics controllers because electrical dynamics change much faster than mechanical dynamics. Another problem is that these methods are designed using a direct-quadrature (DQ) transformation. DQ transformation has been used for commutation in the control of PMSMs [22]. However, such a commutation is not exact because of the time delay of the position and current sensors. The commutation delay causes strikingly qualitative changes in motor behavior [23].

Furthermore, the previous methods are designed based on the cascade control concept for both current and position tracking, where currents track the desired currents that generate the torque required by the electrical controller and the position tracker tracks the position required by the mechanical controller. Therefore, the structures of the previous methods are necessarily complex although the stability is guaranteed. Thus, the gain tuning is difficult to obtain the desired control performance for the PMSMs.

This paper proposes a nonlinear optimal position control method with an observer to improve the position tracking performance of a surface mounted PMSM. The proposed method consists of a desired state generator, controller, and nonlinear observer without DQ transformation. The desired states and inputs are derived using the PMSM model. Then, the state feedback controller is designed based on the whole tracking error dynamics including both mechanical and electrical dynamics. The control and observer gains are chosen using an optimal control method. A nonlinear observer is designed to estimate the velocity and load torque. The closed-loop stability is proven using the input-to-state stability. The proposed method is not designed based on the cascade structure. Furthermore, the control and observer gains are chosen using an optimal control method to obtain the desired performance for the PMSMs. Thus, the gains can be easily tuned compared to the previous methods. This approach simplifies the design process such that the control algorithm is suitable for real-time control. The performance of the proposed method is validated via simulations.

2. Model and Review of Classical Control Methods

2.1. Mathematical Model of Surface Mounted PMSM Motor

We use a Clarke transformation [1,22] to transform the three-phase PMSM model into the α-β frame model as follows:

$$\begin{bmatrix} i_\alpha \\ i_\beta \end{bmatrix} = \begin{bmatrix} \frac{2}{3} & -\frac{1}{3} & -\frac{1}{3} \\ 0 & \frac{1}{\sqrt{3}} & -\frac{1}{\sqrt{3}} \end{bmatrix} \begin{bmatrix} i_a \\ i_b \\ i_c \end{bmatrix},$$
$$\begin{bmatrix} v_\alpha \\ v_\beta \end{bmatrix} = \begin{bmatrix} \frac{2}{3} & -\frac{1}{3} & -\frac{1}{3} \\ 0 & \frac{1}{\sqrt{3}} & -\frac{1}{\sqrt{3}} \end{bmatrix} \begin{bmatrix} v_a \\ v_b \\ v_c \end{bmatrix}, \quad (1)$$

where i_a, i_b, i_c, v_a, v_b, and v_c are the phase currents and voltages in the three-phase model and i_α, i_β, v_α, and v_β are the phase currents and voltages, respectively. The α-β frame model of the surface mounded PMSM [1] is

$$\begin{aligned}
\dot{\theta} &= \omega \\
\dot{\omega} &= -\frac{3}{2}\frac{p\Phi}{J} i_\alpha \sin(p\theta) + \frac{3}{2}\frac{p\Phi}{J} i_\beta \cos(p\theta) - \frac{B}{J}\omega - \frac{\tau_L}{J} \\
\dot{i}_\alpha &= -\frac{R}{L} i_\alpha + \frac{p\Phi}{L}\omega \sin(p\theta) + \frac{1}{L} v_\alpha \\
\dot{i}_\beta &= -\frac{R}{L} i_\beta - \frac{p\Phi}{L}\omega \cos(p\theta) + \frac{1}{L} v_\beta
\end{aligned} \tag{2}$$

where θ is the position, ω is the velocity, R is the resistance L is the inductance and Φ is the permanent magnet linkage, B is the motor viscous friction constant, J is the rotor inertia, θ is the rotor position, ω is the rotor speed, p is the number of pairs of rotor poles, and τ_L is the load torque. The goal of the controller is to track the desired position θ_r.

2.2. Review of Control Method Using DQ Transformation

For the simplification of surface-mounded PMSM model (2), DQ transformation [22] is applied as follows:

$$\begin{aligned}
\begin{bmatrix} i_d \\ i_q \end{bmatrix} &= \begin{bmatrix} \cos(p\theta) & \sin(p\theta) \\ -\sin(p\theta) & \cos(p\theta) \end{bmatrix} \begin{bmatrix} i_\alpha \\ i_\beta \end{bmatrix}, \\
\begin{bmatrix} v_d \\ v_q \end{bmatrix} &= \begin{bmatrix} \cos(p\theta) & \sin(p\theta) \\ -\sin(p\theta) & \cos(p\theta) \end{bmatrix} \begin{bmatrix} v_\alpha \\ v_\beta \end{bmatrix}
\end{aligned} \tag{3}$$

where i_d and i_q are the direct and quadrature currents, and v_d and v_q are the direct and quadrature voltages, respectively. The DQ transformation provides a DQ frame model of the surface mounded PMSM, which is as follows:

$$\begin{aligned}
\dot{\theta} &= \omega \\
\dot{\omega} &= \frac{3}{2}\frac{p\Phi}{J} i_q - \frac{B}{J}\omega - \frac{\tau_L}{J} \\
\dot{i}_d &= -\frac{R}{L} i_d + p\omega i_q + \frac{1}{L} v_d \\
\dot{i}_q &= -\frac{R}{L} i_q - p\omega i_d - \frac{p\Phi}{L}\omega + \frac{1}{L} v_q.
\end{aligned} \tag{4}$$

A block diagram of the general control method using the DQ transformation is shown in Figure 1. In Figure 1, θ_r denotes the reference position. As shown in Figure 1, the DQ transformation also involves an inverse DQ transformation. The structure of the system will be simpler if the controller is designed without a DQ transformation. Generally, PI controllers are used for both mechanical and electrical dynamics.

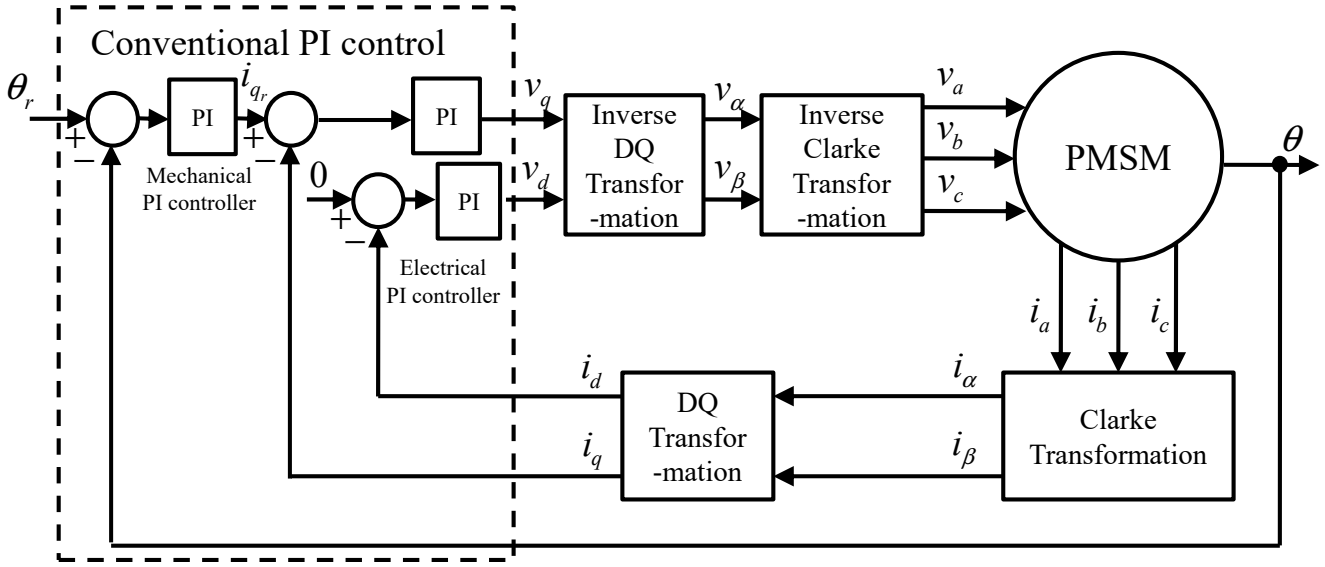

Figure 1. Block diagram of the general control method using DQ transformation.

3. Position Tracking Controller Design

In this section, we develop a position controller for the PMSM. The proposed controller consists of a mechanical controller, a commutation scheme, an electrical controller, and a load torque observer.

3.1. Desired State Design

From the PMSM dynamics (2), the desired PMSM dynamics for the desired position θ_r can be obtained as

$$\begin{aligned}
\dot{\theta}_r =& \omega_r \\
\dot{\omega}_r =& -\frac{3}{2}\frac{p\Phi}{J} i_{\alpha_r} \sin(p\theta_r) + \frac{3}{2}\frac{p\Phi}{J} i_{\beta_r} \cos(p\theta_r) - \frac{B}{J}\omega_r - \frac{\tau_L}{J} \\
\dot{i}_{\alpha_r} =& -\frac{R}{L} i_{\alpha_r} + \frac{p\Phi}{L}\omega_r \sin(p\theta_r) + \frac{1}{L} v_{\alpha_r} \\
\dot{i}_{\beta_r} =& -\frac{R}{L} i_{\beta_r} - \frac{p\Phi}{L}\omega_r \cos(p\theta_r) + \frac{1}{L} v_{\beta_r}
\end{aligned} \tag{5}$$

where ω_r is the velocity, and i_{α_r}, i_{β_r}, v_{α_r}, and v_{β_r} are the desired phase currents and voltages, respectively. In ω_r dynamics of (5), the term $-\frac{3}{2}\frac{p\Phi}{J} i_{\alpha_r} \sin(p\theta_r) + \frac{3}{2}\frac{p\Phi}{J} i_{\beta_r} \cos(p\theta_r)$ corresponds to the desired torque τ_r, which is yet to be defined. To obtain $\tau_r = -\frac{3}{2}\frac{p\Phi}{J} i_{\alpha_r} \sin(p\theta_r) + \frac{3}{2}\frac{p\Phi}{J} i_{\beta_r} \cos(p\theta_r)$, the desired currents i_{α_r} and i_{β_r} are derived as

$$\begin{aligned}
i_{\alpha_r} &= -\frac{2\tau_r}{3p\Phi} \sin(p\theta_r) \\
i_{\beta_r} &= \frac{2\tau_r}{3p\Phi} \cos(p\theta_r).
\end{aligned} \tag{6}$$

Substituting (6) into ω_r dynamics of (5), the dynamics of ω_r becomes

$$\dot{\omega}_r = \frac{3}{2}\frac{p\Phi}{J}\tau_r - \frac{B}{J}\omega_r - \frac{\tau_L}{J}. \tag{7}$$

From the desired PMSM dynamics (5), the desired voltages v_{α_r}, and v_{β_r} are obtained as

$$\begin{aligned} v_{\alpha_r} &= Ri_{\alpha_r} - p\Phi\omega_r \sin(p\theta_r) + L\dot{i}_{\alpha_r} \\ v_{\beta_r} &= Ri_{\beta_r} + p\Phi\omega_r \cos(p\theta_r) + L\dot{i}_{\beta_r}. \end{aligned} \tag{8}$$

3.2. Controller Design

The tracking error $e = \begin{bmatrix} e_I & e_\theta & e_\omega & e_\alpha & e_\beta \end{bmatrix}^T$ is defined as

$$\begin{aligned} e_I &= \int_0^t e_1 d\tau \\ e_\theta &= \theta_r - \theta \\ e_\omega &= \omega_r - \omega \\ e_\alpha &= i_{\alpha_r} - i_\alpha \\ e_\beta &= i_{\beta_r} - i_\beta \end{aligned} \tag{9}$$

where the integrator e_I is used to suppress the steady-state error. From (2) and (9), the tracking error dynamics can be obtained as

$$\begin{aligned} \dot{e}_I &= e_\theta \\ \dot{e}_\theta &= e_\omega \\ \dot{e}_\omega &= \frac{3}{2}\frac{p\Phi}{J}\tau_r - \left[-\frac{3}{2}\frac{p\Phi}{J} i_\alpha \sin(p\theta) + \frac{3}{2}\frac{p\Phi}{J} i_\beta \cos(p\theta)\right] - \frac{B}{J} e_\omega \\ \dot{e}_\alpha &= -\frac{R}{L} e_\alpha + \frac{p\Phi}{L}\omega_r \sin(p\theta_r) + \frac{1}{L} v_{\alpha_r} - \frac{p\Phi}{L}\omega \sin(p\theta) - \frac{1}{L} v_\alpha \\ \dot{e}_\beta &= -\frac{R}{L} e_\beta - \frac{p\Phi}{L}\omega_r \cos(p\theta_r) + \frac{1}{L} v_{\beta_r} + \frac{p\Phi}{L}\omega \cos(p\theta) - \frac{1}{L} v_\beta. \end{aligned} \tag{10}$$

The desired torque τ_r and the desired voltages v_{α_r}, and v_{β_r} are then designed to make the tracking error dynamics (10) be the linear system as

$$\begin{aligned} \tau_r &= \frac{2}{3}\frac{J}{p\Phi}\left[-\frac{3}{2}\frac{p\Phi}{J} i_\alpha \sin(p\theta) + \frac{3}{2}\frac{p\Phi}{J} i_\beta \cos(p\theta) + k_\alpha e_\alpha + k_\beta e_\beta\right] \\ v_\alpha &= p\Phi\omega_r \sin(p\theta_r) - p\Phi\omega \sin(p\theta) + v_{\alpha_r} - Lu_\alpha \\ v_\beta &= -p\Phi\omega_r \cos(p\theta_r) + p\Phi\omega \cos(p\theta) + v_{\beta_r} - Lu_\beta \end{aligned} \tag{11}$$

where u_α and u_β are yet to be defined. With (11), the tracking error dynamics (10) become

$$\begin{aligned} \dot{e}_I &= e_\theta \\ \dot{e}_\theta &= e_\omega \\ \dot{e}_\omega &= k_\alpha e_\alpha + k_\beta e_\beta - \frac{B}{J} e_\omega \\ \dot{e}_\alpha &= -\frac{R}{L} e_\alpha + u_\alpha \\ \dot{e}_\beta &= -\frac{R}{L} e_\beta + u_\beta. \end{aligned} \tag{12}$$

The tracking error dynamics (12) can be rewritten as

$$\underbrace{\begin{bmatrix} \dot{e}_I \\ \dot{e}_\theta \\ \dot{e}_\omega \\ \dot{e}_\alpha \\ \dot{e}_\beta \end{bmatrix}}_{\dot{e}} = \underbrace{\begin{bmatrix} 0 & 1 & 0 & 0 & 0 \\ 0 & 0 & 1 & 0 & 0 \\ 0 & 0 & -\frac{B}{J} & k_\alpha & k_\beta \\ 0 & 0 & 0 & -\frac{R}{L} & 0 \\ 0 & 0 & 0 & 0 & -\frac{R}{L} \end{bmatrix}}_{A_e} \underbrace{\begin{bmatrix} e_I \\ e_\theta \\ e_\omega \\ e_\alpha \\ e_\beta \end{bmatrix}}_{e} + \underbrace{\begin{bmatrix} 0 & 0 \\ 0 & 0 \\ 0 & 0 \\ 1 & 0 \\ 0 & 1 \end{bmatrix}}_{B_e} \underbrace{\begin{bmatrix} u_\alpha \\ u_\beta \end{bmatrix}}_{u} \tag{13}$$

The control input u is designed via the state feedback as

$$u = -K_e e \tag{14}$$

where K_e is the control gain matrix. If K_e is chosen such that $A_e - B_e K_e$ is Hurwitz, then the origin of the error dynamics (13) is exponentially stable.

3.3. Control Gain Selection Using Optimal Control

For the gain tuning guide, the LQR method is applied to the state feedback controller (14). Because the tracking error dynamics (13) is controllable, the LQR method can be applied to it. The cost function is defined as

$$J_c = \int_0^t \left(e^T Q_c e + u^T R_c u \right) d\tau. \tag{15}$$

where Q_c and R_c are positive definite. To obtain the control gain for optimal control, the Riccati equation is used as follows:

$$\begin{aligned} &A_e^T P_c + P_c A_e - P_c B_e B_e^T P_c + Q_c = 0, \\ &K_e = -R_c^{-1} B_e^T P_c. \end{aligned} \tag{16}$$

Generally, Q_c and R_c are chosen to be diagonal for easy gain tuning. Then, $Q_c(1,1)$ in Q_c is chosen to be relatively large compared to others for the position control. When the maximum velocity is slow in the reference position, R_c is chosen to be relatively small compared to the Q_c for the improvement of the position tracking performance. On the other hand, when the maximum velocity is fast in the reference position, R_c is chosen to be relatively large compared to the Q_c for the avoidance of the input saturation.

3.4. Nonlinear Observer

In the design of controller (7), (8), (11), and (14), the speed and the load torque are assumed to be known. In reality, it is difficult to exactly know the velocity and the load torque. To estimate the velocity and load torque, a nonlinear observer is designed as

$$\begin{aligned} \dot{\hat{\theta}} =& \hat{\omega} + l_1(\theta - \hat{\theta}) \\ \dot{\hat{\omega}} =& -\frac{3}{2}\frac{p\Phi}{J} i_\alpha \sin(p\theta) + \frac{3}{2}\frac{p\Phi}{J} i_\beta \cos(p\theta) - \frac{B}{J}\hat{\omega} - \frac{\hat{\tau}_L}{J} \\ &+ l_2(\theta - \hat{\theta}) \\ \dot{\hat{\tau}}_l =& l_3(\theta - \hat{\theta}) \end{aligned} \tag{17}$$

where $\hat{\theta}$, $\hat{\omega}$, and $\hat{\tau}_L$ are the estimated position, velocity, and load torque, respectively, and l_1, l_2, and l_3 are the observer gains. The estimation errors are defined as

$$\tilde{x} = \begin{bmatrix} \tilde{\theta} \\ \tilde{\omega} \\ \tilde{\tau}_L \end{bmatrix} = \begin{bmatrix} \theta - \hat{\theta} \\ \omega - \hat{\omega} \\ \tau_L - \hat{\tau}_L \end{bmatrix}. \tag{18}$$

The estimation error dynamics are

$$\underbrace{\begin{bmatrix}\dot{\tilde{\theta}}\\ \dot{\tilde{\omega}}\\ \dot{\tilde{\tau}}_l\end{bmatrix}}_{\dot{\tilde{x}}} = \underbrace{\begin{bmatrix}-l_1 & 1 & 0\\ -l_2 & -\frac{B}{J} & -\frac{1}{J}\\ -l_3 & 0 & 0\end{bmatrix}}_{A_o}\underbrace{\begin{bmatrix}\tilde{\theta}\\ \tilde{\omega}\\ \tilde{\tau}_L\end{bmatrix}}_{\tilde{x}}. \tag{19}$$

If l_1, l_2, and l_3 are chosen such that A_o is Hurwitz, then the origin of the estimation error dynamics (19) is exponentially stable.

3.5. Observer Gain Selection Using Optimal Control

For the gain tuning guide, the LQR method is applied to the observer (17). The estimation error dynamics can be rewritten as

$$\underbrace{\begin{bmatrix}\dot{\tilde{\theta}}\\ \dot{\tilde{\omega}}\\ \dot{\tilde{\tau}}_l\end{bmatrix}}_{\dot{\tilde{x}}} = \left(\underbrace{\begin{bmatrix}0 & 1 & 0\\ 0 & -\frac{B}{J} & -\frac{1}{J}\\ 0 & 0 & 0\end{bmatrix}}_{A_{o_1}} - \underbrace{\begin{bmatrix}l_1\\ l_2\\ l_3\end{bmatrix}}_{L_o}\underbrace{\begin{bmatrix}1 & 0 & 0\end{bmatrix}}_{C_o}\right)\underbrace{\begin{bmatrix}\tilde{\theta}\\ \tilde{\omega}\\ \tilde{\tau}_L\end{bmatrix}}_{\tilde{x}}. \tag{20}$$

Because the estimation error dynamics (20) is observable, the LQR method can be applied to it. The cost function is defined as

$$J_o = \int_0^t \left(\tilde{x}^T Q_o \tilde{x} + u^T R_o u\right) d\tau. \tag{21}$$

where Q_o and R_o are positive definite. To obtain the observer gain for optimal control, the Riccati equation is used as follows:

$$\begin{aligned} &A_{o_1}P_o + P_o A_{o_1}^T - P_o C_o^T C_o P_o + Q_o = 0,\\ &L_o = -R_o^{-1} C_o P_o. \end{aligned} \tag{22}$$

3.6. Closed-Loop System Stability Analysis

The stability of the tracking error dynamics in (13) is proven under an assumption that the velocity and load torque are known. With regard to the estimation error dynamics in (19), the closed-loop system can be derived as

$$\begin{aligned} \underbrace{\begin{bmatrix}\dot{e}_I\\ \dot{e}_\theta\\ \dot{e}_\omega\\ \dot{e}_\alpha\\ \dot{e}_\beta\end{bmatrix}}_{\dot{e}} &= \underbrace{\begin{bmatrix}0 & 1 & 0 & 0 & 0\\ 0 & 0 & 1 & 0 & 0\\ 0 & 0 & -\frac{B}{J} & k_\alpha & k_\beta\\ 0 & 0 & 0 & -\frac{R}{L} & 0\\ 0 & 0 & 0 & 0 & -\frac{R}{L}\end{bmatrix}}_{A_e}\underbrace{\begin{bmatrix}e_I\\ e_\theta\\ e_\omega\\ e_\alpha\\ e_\beta\end{bmatrix}}_{e} + \underbrace{\begin{bmatrix}0 & 0\\ 0 & 0\\ 0 & 0\\ 1 & 0\\ 0 & 1\end{bmatrix}}_{B_e}\underbrace{\begin{bmatrix}u_\alpha\\ u_\beta\end{bmatrix}}_{u} + \underbrace{\begin{bmatrix}0 & 0 & 0\\ 0 & \frac{B}{J} & 0\\ 0 & 0 & \frac{1}{J}\\ 0 & -\frac{p\Phi}{L}\sin(p\theta) & 0\\ 0 & \frac{p\Phi}{L}\cos(p\theta) & 0\end{bmatrix}}_{B_{est}}\underbrace{\begin{bmatrix}\tilde{\theta}\\ \tilde{\omega}\\ \tilde{\tau}_L\end{bmatrix}}_{\tilde{x}}\\ \underbrace{\begin{bmatrix}\dot{\tilde{\theta}}\\ \dot{\tilde{\omega}}\\ \dot{\tilde{\tau}}_l\end{bmatrix}}_{\dot{\tilde{x}}} &= \underbrace{\begin{bmatrix}-l_1 & 1 & 0\\ -l_2 & -\frac{B}{J} & -\frac{1}{J}\\ -l_3 & 0 & 0\end{bmatrix}}_{A_3}\underbrace{\begin{bmatrix}\tilde{\theta}\\ \tilde{\omega}\\ \tilde{\tau}_L\end{bmatrix}}_{\tilde{x}}. \end{aligned} \tag{23}$$

With the control law $u = -K_e e$ (14), the closed-loop system can be rewritten by

$$\begin{aligned} \dot{e} &= (A_e - B_e K_e)e + B_{est}\tilde{x}\\ \dot{\tilde{x}} &= A_o \tilde{x}. \end{aligned} \tag{24}$$

Because $(A_e - B_e K_e)$ is Hurwitz and B_{est} is bounded, the dynamics of e are input-to-state stable. With Hurwitz A_o, $\tilde{x}$ exponentially converges to zero. Thus, e also converges to zero. We conclude that the closed-loop system (24) is stable.

A block diagram of the proposed method is presented in Figure 2. The nonlinear observer (18) estimates the velocity and load torque using the position and current feedback. Then, desired states and inputs are derived using (6), (7), (9), and (12). The the control inputs (12) are obtained with the optimal state feedback control (15) and (17).

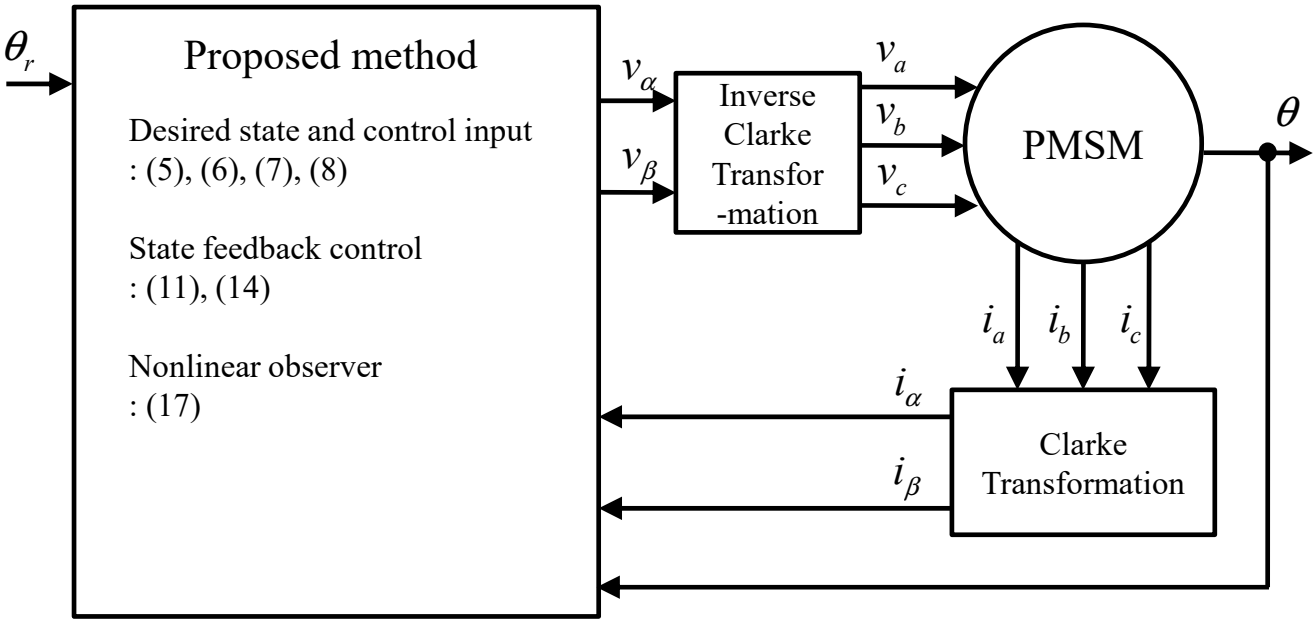

Figure 2. Block diagram of the proposed method.

4. Simulation and Experimental Results

Simulations and experiments were tested to validate the performance of the proposed method. The parameters listed in Table 1 were used. The control gains were obtained using $Q_c = diag(0.5, 500, 000, 5000, 100, 100)$, $R_c = diag(1, 1)$, $Q_o = diag(50, 10, 10)$, and $R_o = diag(1, 1)$ The desired position $\theta_r(t) = sin(\pi t)(1 + e^{-10t})$ used in the simulations is shown in Figure 3.

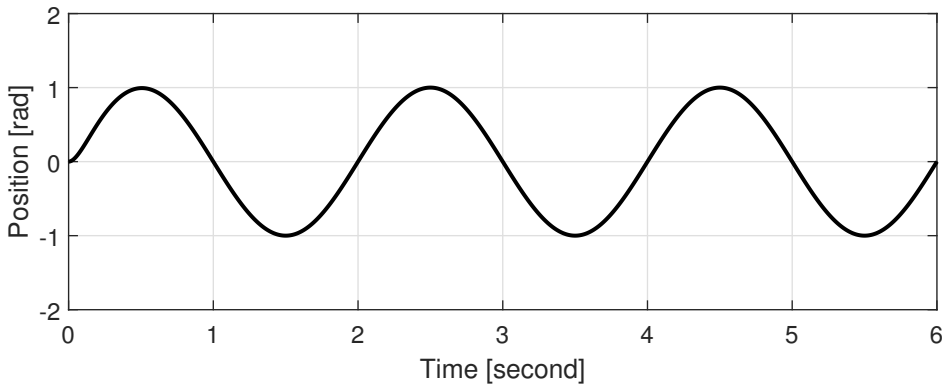

Figure 3. Desired position.

Table 1. PMSM Parameters.

Para.	Value	Para.	Value
L	11 mH	R	0.12 Ω
Φ	0.18 V·s/rad	J	0.006 Kg·m^2
p	3	B	0.001 N·m· s/rad

4.1. Simulations

The simulations were performed to evaluate the performance of the proposed controller. The load torque was 0.5 Nm. The position and velocity tracking errors of the PI controller and the proposed method were shown in Figures 4 and 5, respectively. The position and velocity tracking errors of the PI controller were relatively larger than those of the proposed method. Furthermore, a large peak appeared in the velocity of the PI controller. This resulted in the large peak of the position of the PI controller. On the other hand, the position and velocity tracking errors converged to zeros rapidly. Furthermore, the position and velocity tracking errors of the proposed method were smaller than those of the PI controller in the steady-state responses. We conclude that the position and velocity tracking performances were improved by the proposed method. Figure 6 shows the load torque estimation performance of the nonlinear observer. The estimated load torque satisfactorily followed the actual load torque.

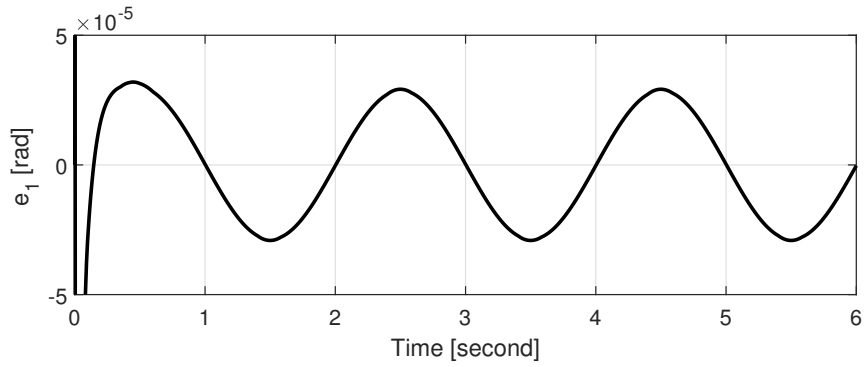

(**a**) Position tracking error e_1

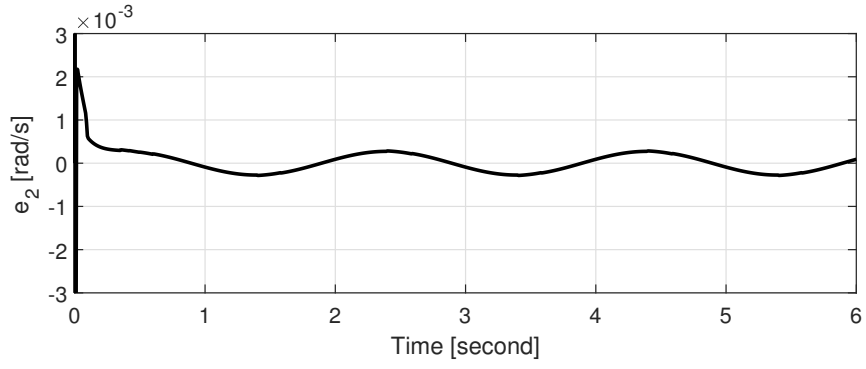

(**b**) Velocity tracking error e_2

Figure 4. Position and velocity tracking errors of the PI controller.

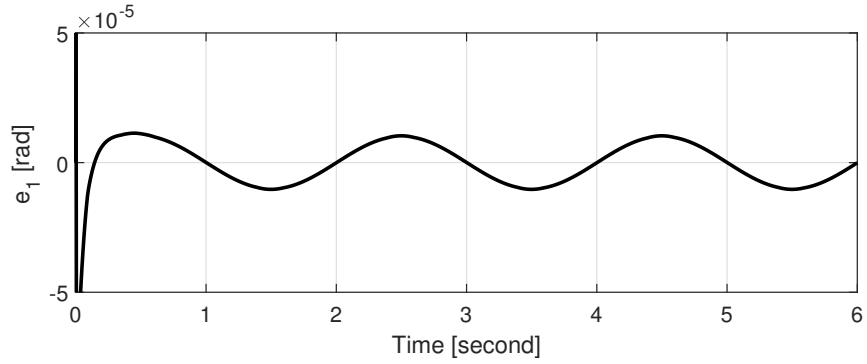

(**a**) Position tracking error e_1

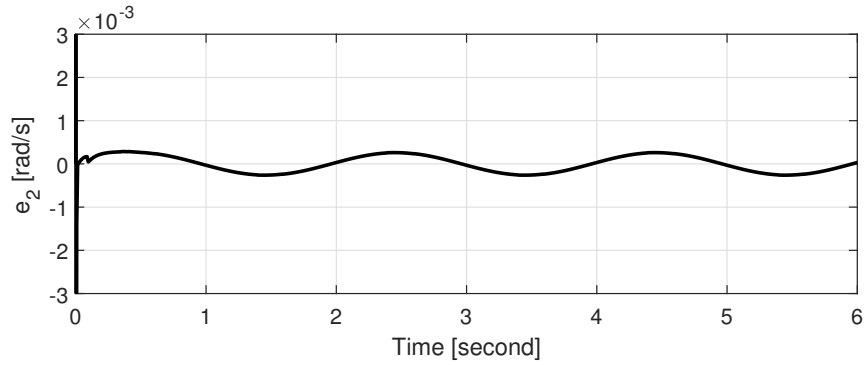

(**b**) Velocity tracking error e_2

Figure 5. Position and velocity tracking errors of the proposed method.

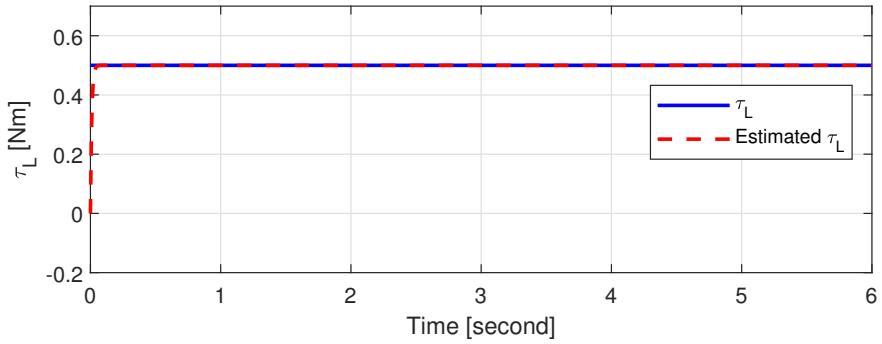

Figure 6. Load torque estimation performance of the nonlinear observer.

4.2. Experiments

The experiments were performed to evaluate the performance of the proposed method. The proposed method was compared with the PI controller and the backstepping method. The PI control method shown in Figure 1 was used to compare the position tracking performance. For a fair performance comparison, a feedforward term to compensate for the load torque was added to the mechanical dynamics controller as follows:

$$i_{q_r} = K_{p\omega} e_\omega + K_{i\omega} \int_0^t e_\omega d\tau + \frac{2}{3p\Phi} \hat{\tau}_L \tag{25}$$

where $K_{p\omega}$ and $K_{i\omega}$ are the control gains. The control gains of the PI controller were chosen by using the method [24]. The backstepping method proposed in [25] was used in the experiments. Experimental setup is shown in Figure 7. The proposed method and the PI controller were coded in C Language using TMS320F2808. A surface-mounted PMSM (APM-SB03ADK-9) produced by Kwapil & Co was used. An encoder (2500 pulses per

revolution) coupled to the PMSM was used to obtain the position. The sampling rate was set to be 5 kHz. The currents were measured by the current sensors embedded in the motor drive. Twelve-bit analog to digital (A/D) converters and 12-bit digital to analog (D/A) converters were used. The power supply (±24) was used. The motor coupled to the PMSM was used to generate the load torque.

The position tracking performances of three methods are shown in Figure 8. Due to the friction, the relatively large position tracking error appeared near zero velocity in three methods. After the zero velocity period, the position tracking errors were reduced by the backstepping method and the proposed method. Furthermore, the ripples were reduced by the backstepping method and the proposed method. Because the desired state values generated by the system modeling and the optimal tuned gains were used in the proposed method, The position tracking error of the proposed method was relatively smaller than that of the backsteppig method. The unavoidable position ripples appeared due to the encoder coupling effect, PWM driver noise, modeling uncertainty, nonideal sinusoidal flux distribution, and the friction. Figure 9 shows the load torque estimation performance of the nonlinear observer. In practice, it is impossible to generate the square load torque. Furthermore, the estimated load torque may include the nonlinearity of the PWM driver, parameter uncertainty, and the friction as well as the load torque. Thus, the estimated load torque reflected these values in the form of fluctuations as shown in Figure 9.

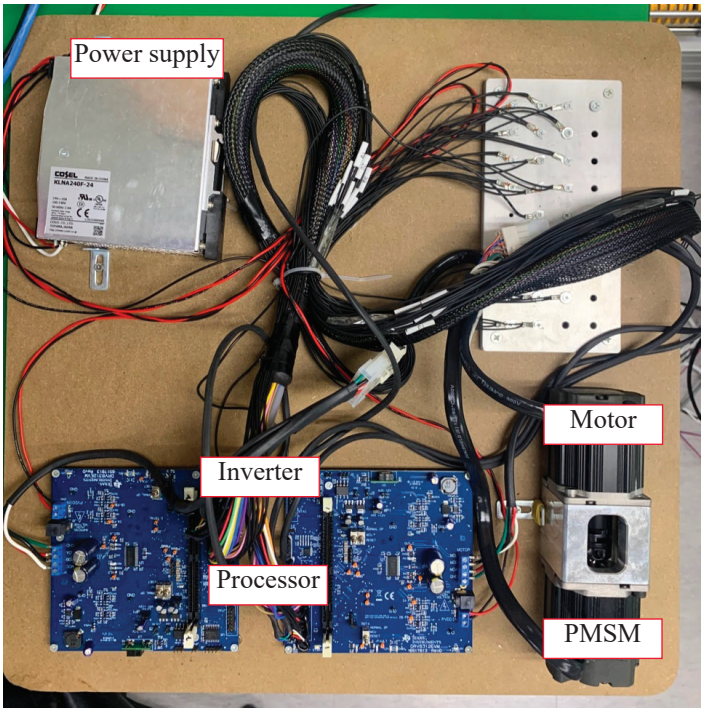

Figure 7. Experimental setup.

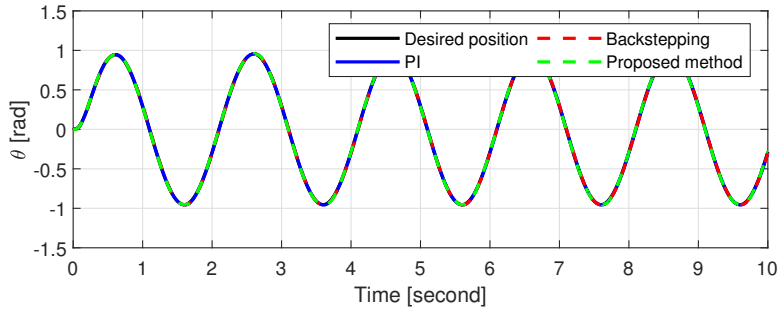

(**a**) Position tracking performance θ

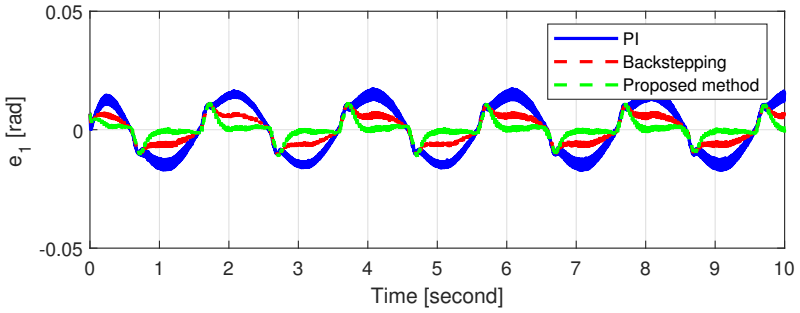

(**b**) Position tracking error e_1

Figure 8. Position tracking performances of the PI controller and the proposed method.

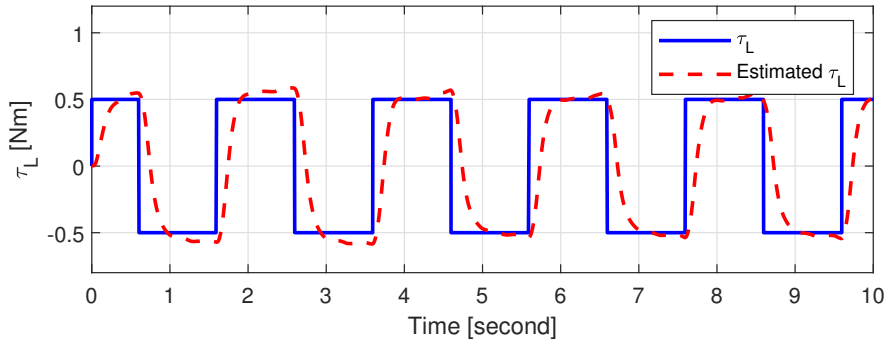

Figure 9. Load torque estimation performance of the nonlinear observer.

5. Conclusions

Here, a nonlinear optimal position control with an observer was developed to improve the position tracking performance of the PMSM. The proposed method consists of a desired state generator, controller, and nonlinear observer. The desired states and inputs were derived using the PMSM model. Then, the state feedback controller was designed based on the tracking error. Control gains were chosen using the optimal control method. A nonlinear observer was designed to estimate the velocity and load torque. The closed-loop stability was proven using input-to-state stability. The performance of the proposed method was validated via simulations and experiments.

Author Contributions: D.H.H. and R.K. designed the algorithm and developed the simulation; D.H.H. and R.K. provided guidance in designing the algorithm; D.H.H. and R.K. verified the simulation model and results. All authors have read and agreed to the published version of the manuscript.

Funding: This research received no external funding.

Institutional Review Board Statement: Not applicable.

Informed Consent Statement: Not applicable.

Data Availability Statement: Not applicable.

Conflicts of Interest: The authors declare no conflicts of interest.

References

1. Bose, B.K. *Power Electronics and AC Drives*; Prentice-Hall: Englewood Cliffs, NJ, USA, 1968.
2. Toliyat, H.A.; Kliman, G.B. *Handbook of Electric Motors*; Marcel Dekker: New York, NY, USA, 2004.
3. Hur, J. Characteristic analysis of interior permanent-magnet synchronous motor in electrohydraulic power steering systems. *IEEE Trans. Ind. Electon.* **2008**, *55*, 2316–2323.
4. Tursini, M.; Parasiliti, F.; Zhang, D. Real-time gain tuning of PI controllers for high-performance PMSM drives. *IEEE Trans. Ind. Appl.* **2002**, *38*, 1018–1026. [CrossRef]
5. GrCar, B.; Cafuta, P.; Znidaric, M.; Gausch, F. Nonlinear Control of Synchronous Servo Drive. *IEEE Trans. Control Syst. Technol.* **1996**, *4*, 177–184. [CrossRef]
6. Baik, I.-C.; Kim, K.-H.; Youn, M.-J. Robust nonlinear speed control of PM synchronous motor using boundary layer integral sliding mode control technique. *IEEE Trans. Control Syst. Technol.* **2000**, *8*, 47–54. [CrossRef]
7. Chung, M.-J.; Gweon, D.-G. Design optimization and development of linear brushless permanent magnet motor. *Int. J. Control. Automa. Syst.* **2003**, *1*, 351–357.
8. Hernandez-Guzman, V.M.; Silva-Ortigoza, R. PI control plus electric current loops for PM synchronous motors. *IEEE Trans. Control Syst. Technol.* **2011**, *19*, 868–873. [CrossRef]
9. Li, S.; Zong, K.; Liu, H. A composite speed controller based on a second-order model of permanent magnet synchronous motor system. *Trans. Insttute Meas. Control* **2011**, *33*, 522–541.
10. Zhang, X.; Zhang, L.; Zhang, Y. Model predictive current control for PMSM drives with parameter robustness improvement. *IEEE Trans. Power Electron.* **2018**, *34*, 1645–1657. [CrossRef]
11. Du, H.; Wen, G.; Cheng, Y.; Lu, J. Design and implementation of bounded finite-time control algorithm for speed regulation of permanent magnet synchronous motor. *IEEE Trans. Ind. Electron.* **2021**, *68*, 2417–2426. [CrossRef]
12. Le, K.M.; Hoang, H.V.; Jeon, J.W. An advanced closed-loop control to improve the performance of hybrid steppermotors. *IEEE Trans. Power Electron.* **2017**, *32*, 7244–7255. [CrossRef]
13. Zhou, Z.; Xia, C.; Yan, Y.; Wang, Z.; Shi, T. Disturbances attenuation of permanent magnet synchronous motor drives using cascaded predictive integral-resonant controllers. *IEEE Trans. Power Electron.* **2018**, *33*, 1514–1527. [CrossRef]
14. Lee, Y.; Gil, J.; Kim, W. Velocity control for sideband harmonics compensation in permanent magnet synchronous motors with low switching frequency inverter. *IEEE Trans. Ind. Electron.* **2021**, *68*, 3434–3444. [CrossRef]
15. Zhu, W.; Chen, D.; Du, H.; Wang, X. Position control for permanent magnet synchronous motor based on neural network and terminal sliding mode control. *Trans. Inst. Meas. Control* **2020**, *42*, 1632–1640. [CrossRef]
16. Xia, C.; Liu, N.; Zhou, Z.; Yan, Y.; Shi, T. Steady-state performance improvement for LQR-based PMSM drives. *IEEE Trans. Power Electron.* **2018**, *33*, 10622–10632. [CrossRef]
17. Alfehaid, A.A.; Strangas, E.G.; Khalil, H.K. Speed control of permanent magnet synchronous motor with uncertain parameters and unknown disturbance. *IEEE Trans. Control Syst. Technol.* **2021**, *29*, 2639–2646. [CrossRef]
18. Kim, W.; Shin, D.; Chung, C.C. The Lyapunov-based controller with a passive nonlinear observer to improve position tracking performance of microstepping in permanent magnet stepper motors. *Automatica* **2012**, *48*, 3064–3074. [CrossRef]
19. Ortega, R.; Praly, L.; Astolfi, A.; Lee, J.; Nam, K. Estimation of rotor position and speed of permanent magnet synchronous motors with guaranteed stability. *IEEE Trans. Control Syst. Technol.* **2010**, *19*, 601–614. [CrossRef]
20. Pauline, B.; Praly, L. Convergence of gradient observer for rotor position and magnet flux estimation of permanent magnet synchronous motors. *Automatica* **2018**, *94*, 88–93.
21. Pyrkin, A.; Bobtsov, A.; Ortega, R.; Vedyakov, A.; Cherginets, D.; Ovcharov, A.; Bazylev, D.; Petranevsky, I. Robust nonlinear observer design for permanent magnet synchronous motors. *IET Control Theory Appl.* **2021**, *15*, 604–616. [CrossRef]
22. Park, R.H. Two-reaction theory of synchronous machines generalized method of analysis. *AIEE Trans.* **1929**, *48*, 716–727. [CrossRef]
23. Krishnamurthy, P.; Khorrami, F. An analysis of the effects of closed-loop commutation delay on stepper motor control and application to parameter estimation. *IEEE Trans. Control Syst. Technol.* **2008**, *16*, 70–77. [CrossRef]
24. Åström, K.J.; Hägglund, T. The future of PID control. Control engineering practice. *Control Eng. Prac.* **2001**, *9*, 1163–1175. [CrossRef]
25. Shin, D.; Kim, W.; Chung, C.C. Position control of a permanent magnet stepper motor by MISO backstepping in semi-strict feedback form. In Proceedings of the 2011 IEEE/ASME International Conference on Advanced Intelligent Mechatronics (AIM), Budapest, Hungary, 3–7 July 2011; pp. 808–813.